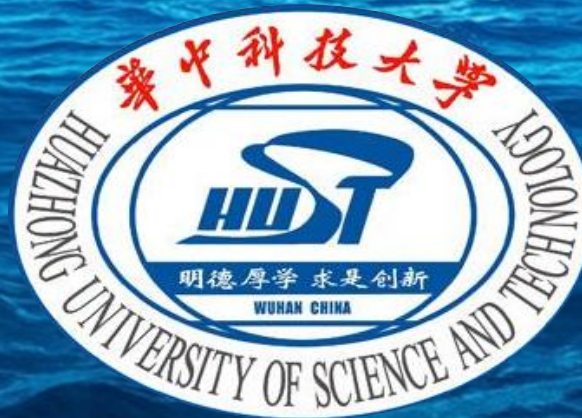


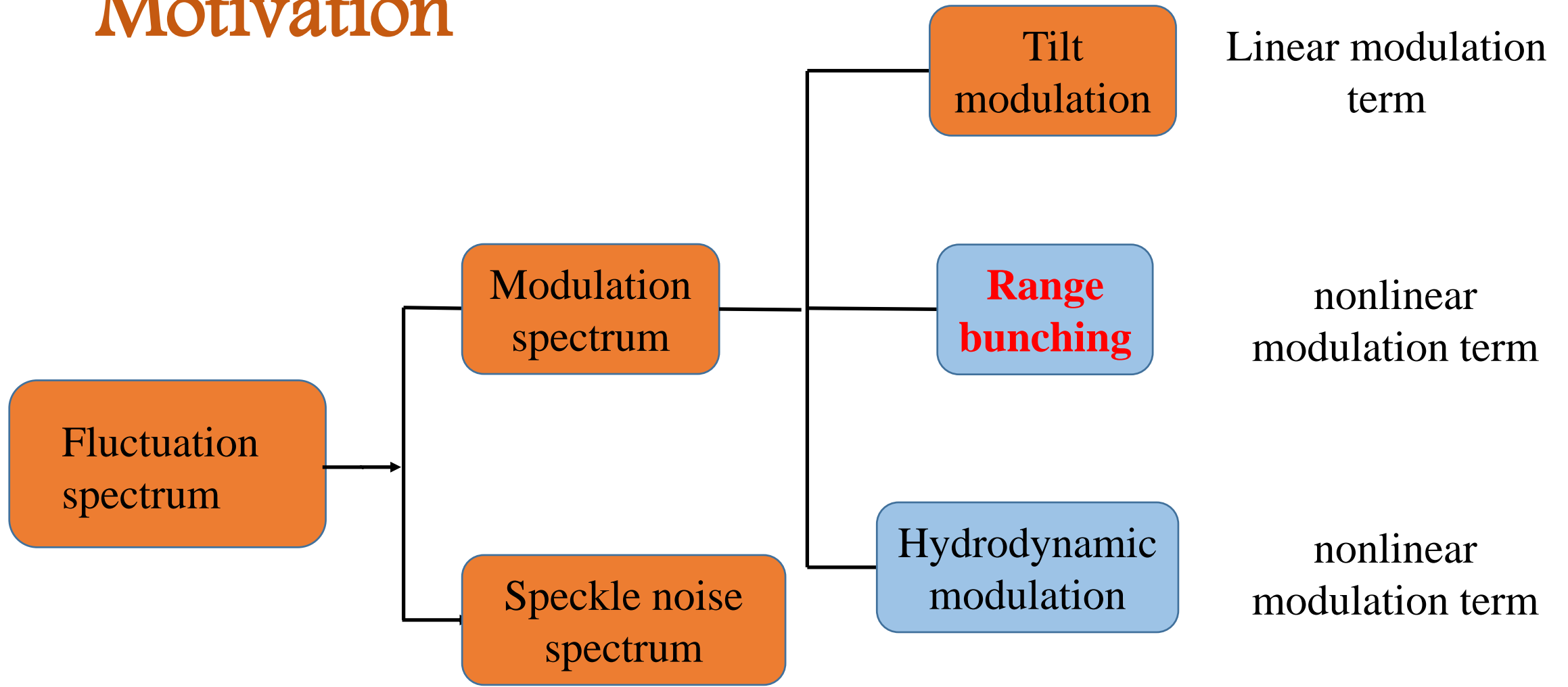
Effects of range bunching on modulation spectrum measured by a wave scatterometer

Jiayang Si and Ping Chen

• [HuaZhong University of Science and Technology](#)



Motivation

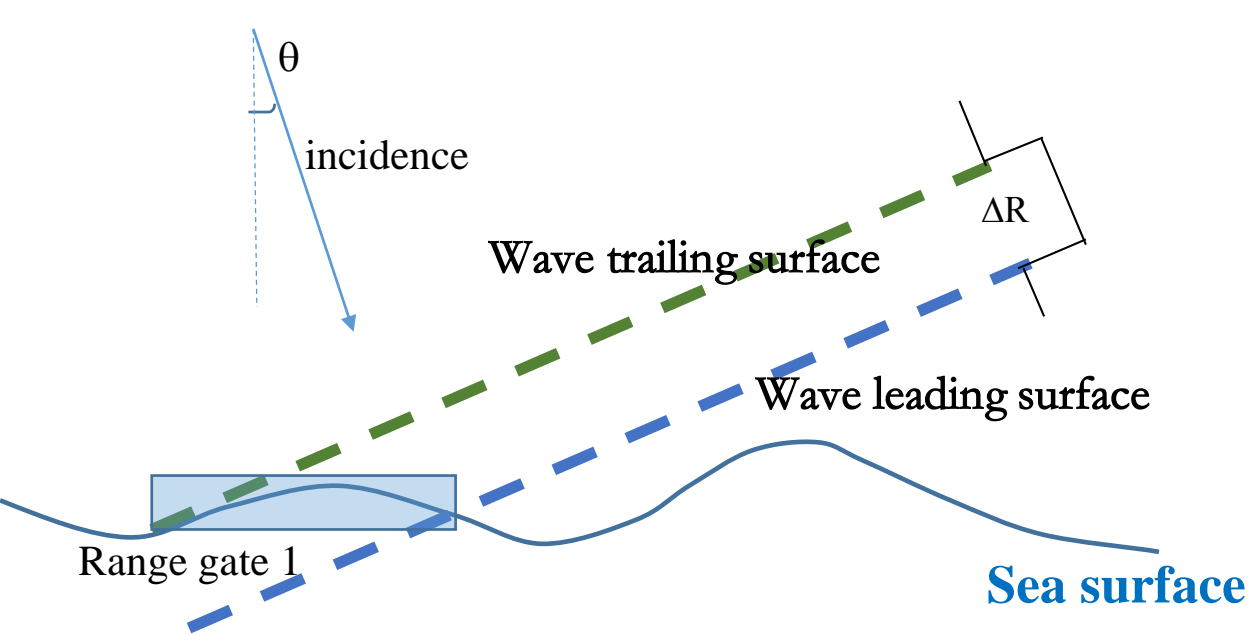


Outlines

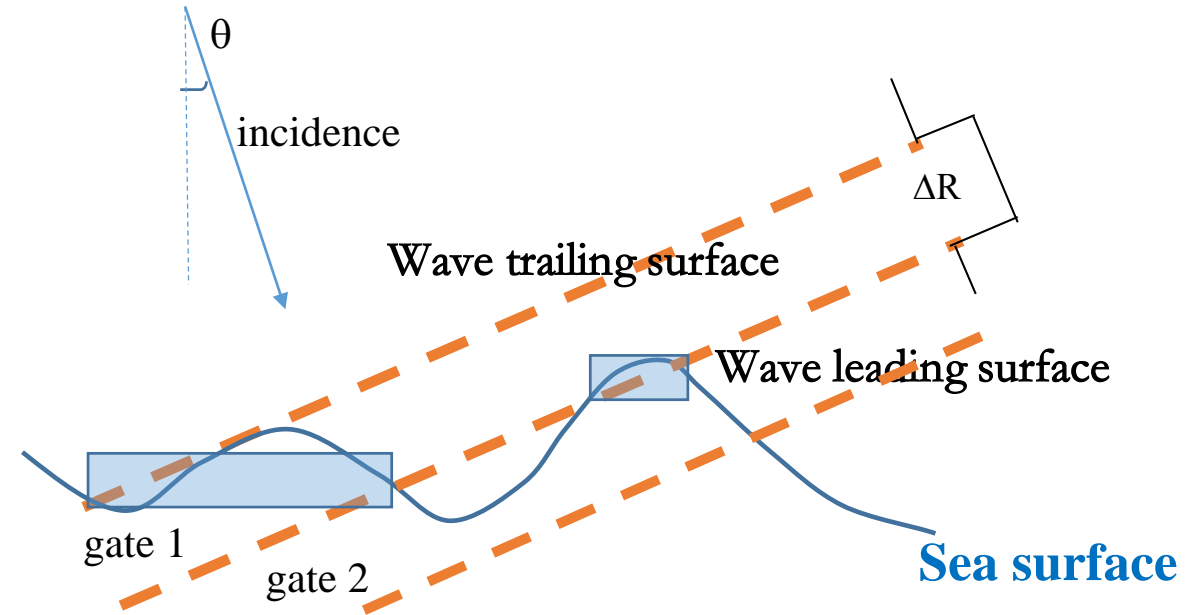
- 1. Range-bunching**
- 2. A modulation spectrum model with range-bunching**
- 3. Effects of range-bunching by the model**
- 4. Conclusion**

Part 1: What is range bunching?

Ideal cases-----without range bunching



Some cases-----with range bunching



Part 2: Modulation spectrum model without/with range-bunching

Linear model (given by Jackson 81) ← Without range-bunching

$$P_m(\vec{K}) = MTF \cdot K^2 F(\vec{K})$$

$$MTF = \frac{\sqrt{2\pi}}{L_y} \alpha^2 \quad \alpha = \cot\theta - \frac{\partial \ln \sigma^0}{\partial \theta}$$

Nonlinear model (given by Jackson 81) ← With range-bunching

$$P'_m(\vec{K}) = \frac{\sqrt{2\pi}}{L_y} e^{-(\vec{K}\sigma\cot\theta)^2} \cdot (P_m(\vec{K}) + \text{nonlinear term})$$

$$\begin{aligned} \text{nonlinear term} = & \frac{1}{2} K^4 \cot^4 \theta F(\vec{K}) * F(\vec{K}) + K^2 \cot^2 \theta \left(\frac{p_{\alpha\beta}}{p} + \frac{p_{\alpha} p_{\beta}}{p^2} \right) \overline{\vec{K}_{\alpha} F(\vec{K})} * \overline{\vec{K}_{\beta} F(\vec{K})} \\ & + \frac{1}{2} \frac{p_{\alpha\delta} p_{\beta\eta}}{p^2} \overline{\vec{K}_{\alpha} \vec{K}_{\beta} F(\vec{K})} * \overline{\vec{K}_{\delta} \vec{K}_{\eta} F(\vec{K})} - 2K^3 \cot^3 \theta \frac{p_{\alpha}}{p} F(\vec{K}) * \overline{\vec{K}_{\alpha} F(\vec{K})} \\ & + K^2 \cot^2 \theta \frac{p_{\alpha} p_{\beta}}{p^2} F(\vec{K}) * \overline{\vec{K}_{\alpha} \vec{K}_{\beta} F(\vec{K})} - K \cot \theta \left(\frac{p_{\alpha} p_{\beta\delta} + p_{\beta} p_{\alpha\delta}}{p^2} \right) \overline{\vec{K}_{\delta} F(\vec{K})} * \overline{\vec{K}_{\alpha} \vec{K}_{\beta} F(\vec{K})} \end{aligned}$$

Part 3: Effects of range-bunching calculated by the model

Use the nonlinear/linear modulation spectrum model to simulate the modulation spectrum P'_m / P_m with/without range-bunching in different sea surface conditions (swell and wind wave) with different incidence angles (2° , 4° , 6° , 8° , 10° , 12°).

The slope spectrum S' / S is inverted from the P'_m / P_m according the linear method.

$$S' = P'_m / \text{MTF},$$

$$S = P_m / \text{MTF}$$

The wave height spectrum is calculated, and the significant height H_s and the peak wave length are obtained.

Part 3: Effects of range-bunching calculated by the model

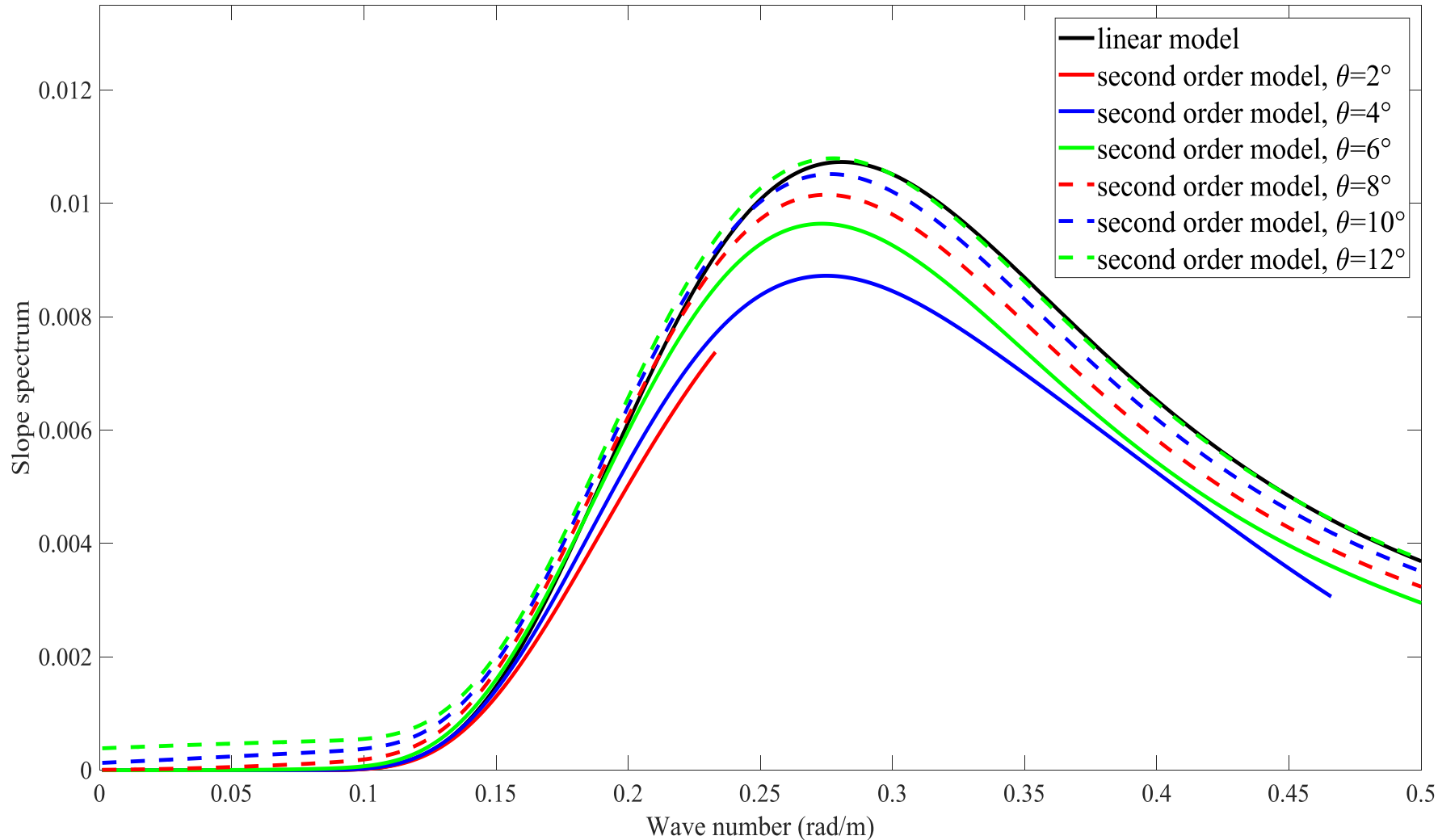
Observed along the wave direction

along wave direction
WS=8m/s, $\Omega=1.3$

Developing wind wave

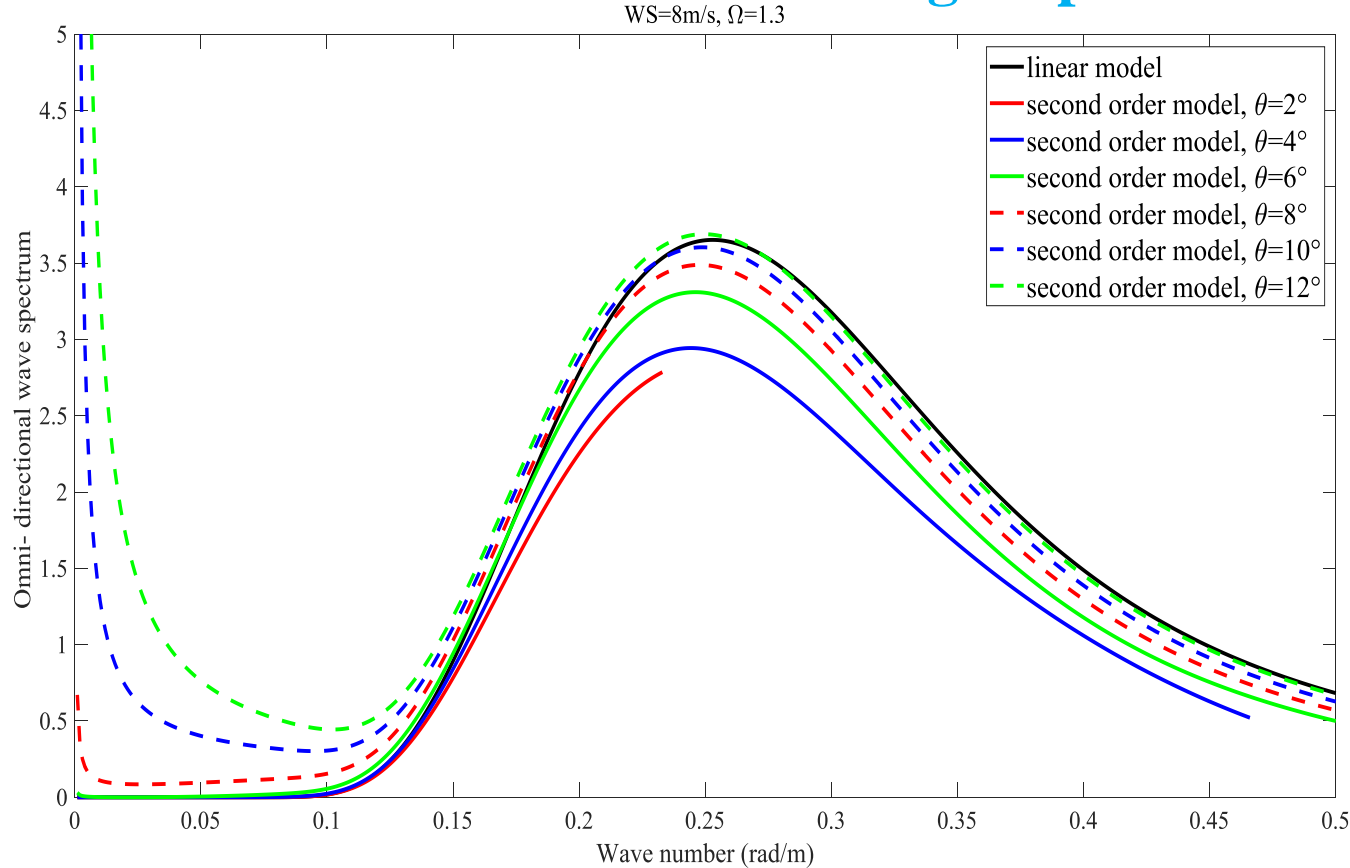
$$U_{10} = 8 \text{ m/s} \quad \Omega = 1.3$$

With the incidence angle decreasing, the **attenuation** of the spectrum become larger, the **peak wavenumber shift to the left** slightly



Part 3: Effects of range-bunching calculated by the model

Omni-directional wave height spectrum



Developing wind wave

$$U_{10} = 8 \text{ m/s} \quad \Omega = 1.3$$

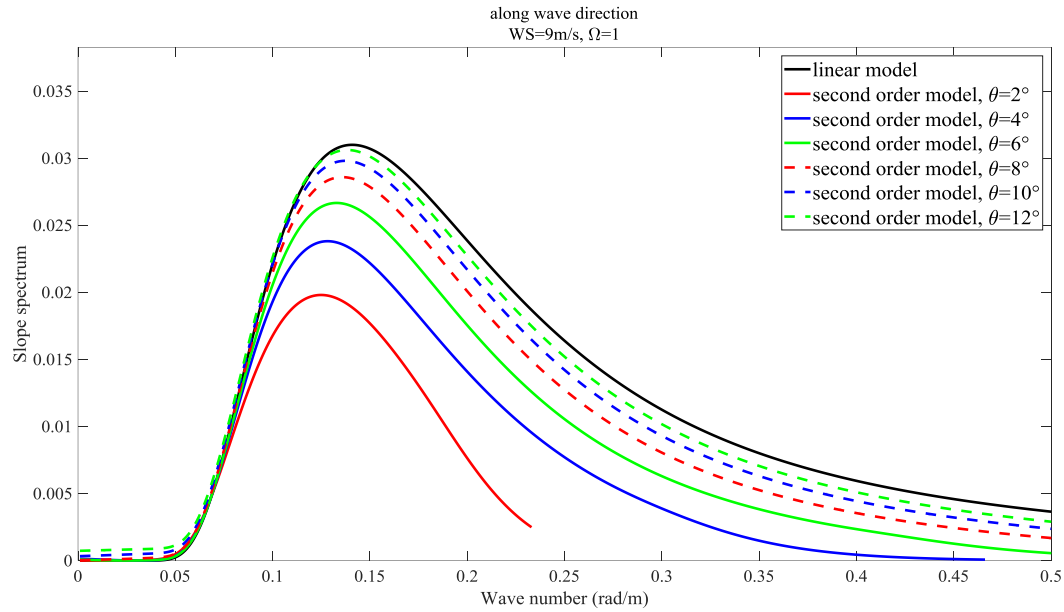
	Inversed Hs (m)	Relative error (%)	Inversed λ_p (m)	Relative error (%)
Linear model	0.72	~	24.8	~
2°	~	~	~	~
4°	~	~	25.8	+4.0
6°	0.64	-11.1	25.5	+2.8
8°	0.68	-5.6	25.3	+2.0
10°	0.73	+1.4	25.2	+1.6
12°	0.79	+9.7	25.2	+1.6

With the incidence angle decreasing, the attenuation of the spectrum become larger.

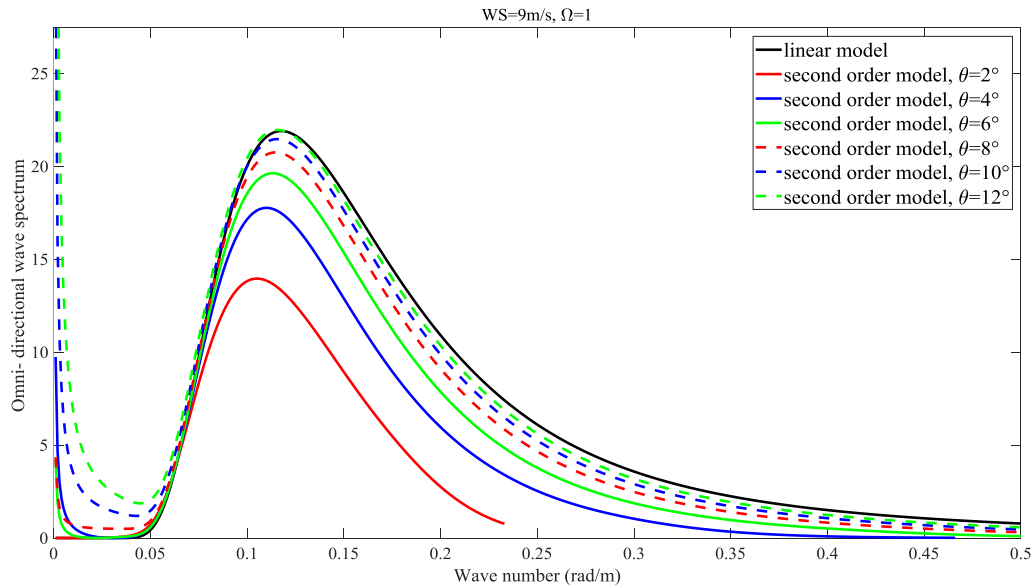
With the incidence angle increasing (above 8°), the parasitic peaks at low wave number become larger. **It shows that range-bunching is an important factor leading to parasitic peaks at low wave number in inverted wave height spectrum.**

The inverted Hs may be the result of the superposition of the pseudo-peak in low wave number and the spectral attenuation of other parts.

Observed along
the wave
direction



Omnidirectional
wave height
spectrum

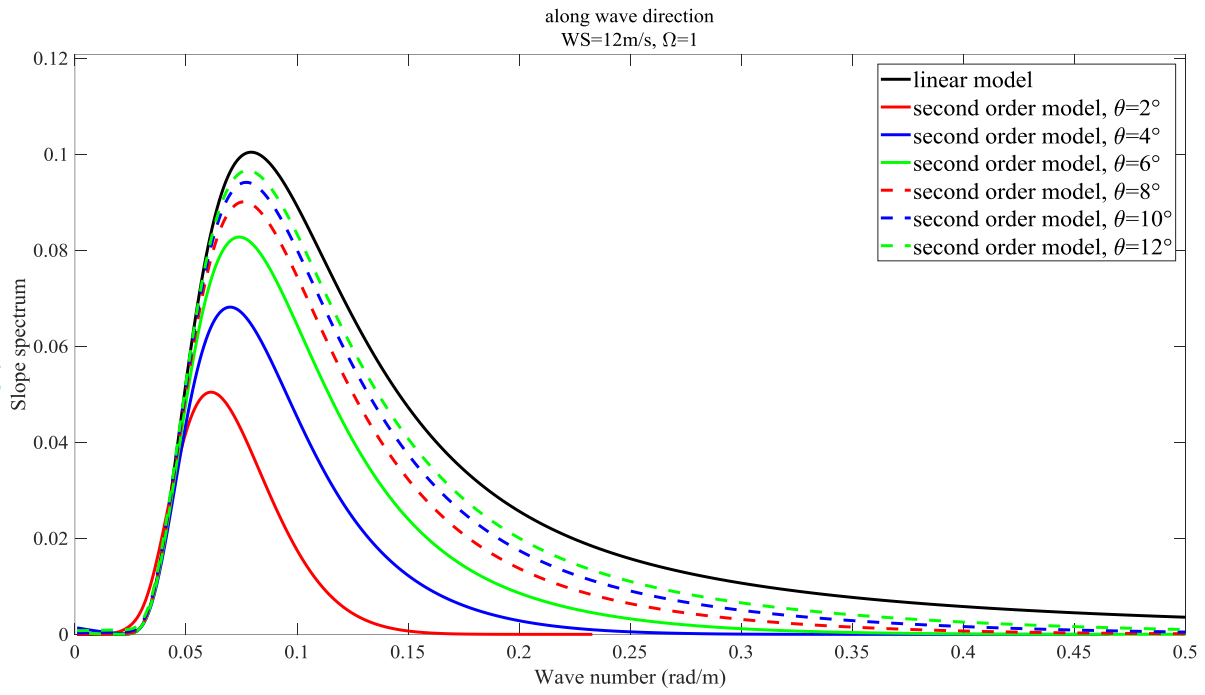


mature wind wave

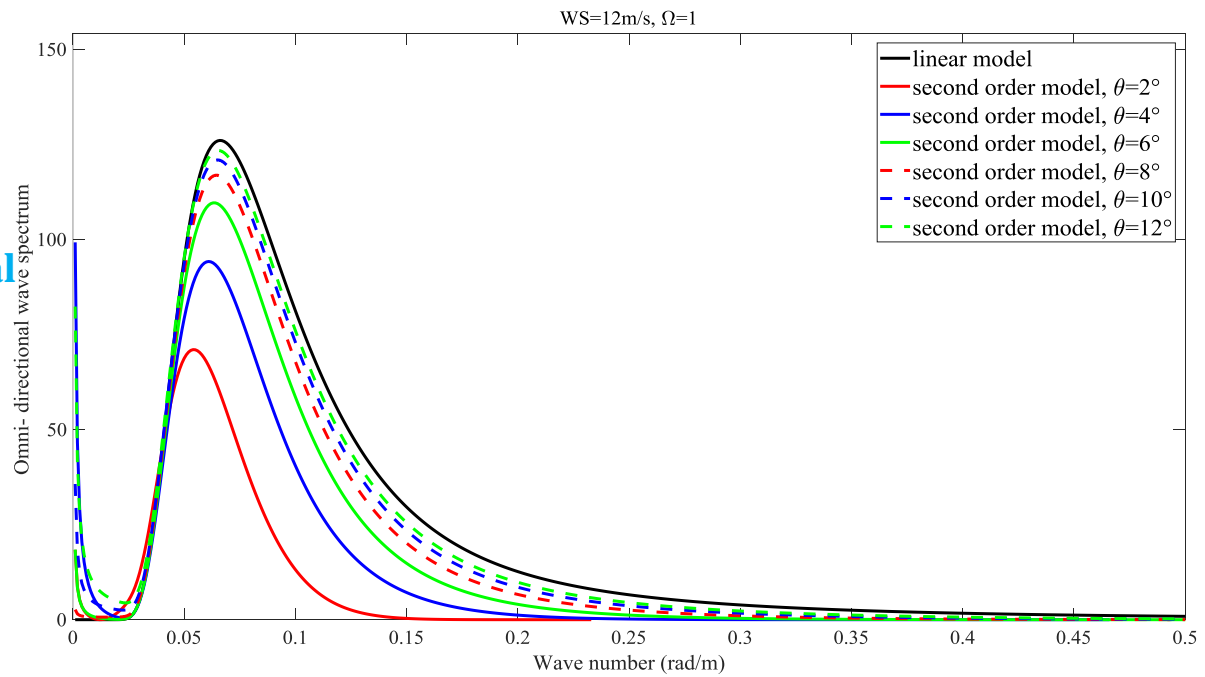
$$U_{10} = 9 \text{ m/s} \quad \Omega = 1$$

	Inversed Hs (m)	Relative error (%)	Inversed λ_p (m)	Relative error (%)
Linear model	1.38	~	53.2	~
2°	~	~	59.8	+ 12.4
4°	1.08	- 21.7	57.1	+ 7.3
6°	1.19	- 13.8	55.6	+ 4.5
8°	1.27	- 8.0	54.6	+ 2.6
10°	1.35	- 2.2	54.6	+ 2.6
12°	1.41	+ 2.2	54.2	+ 2.6

Observed along
the wave
direction



Omnidirectional
wave height
spectrum

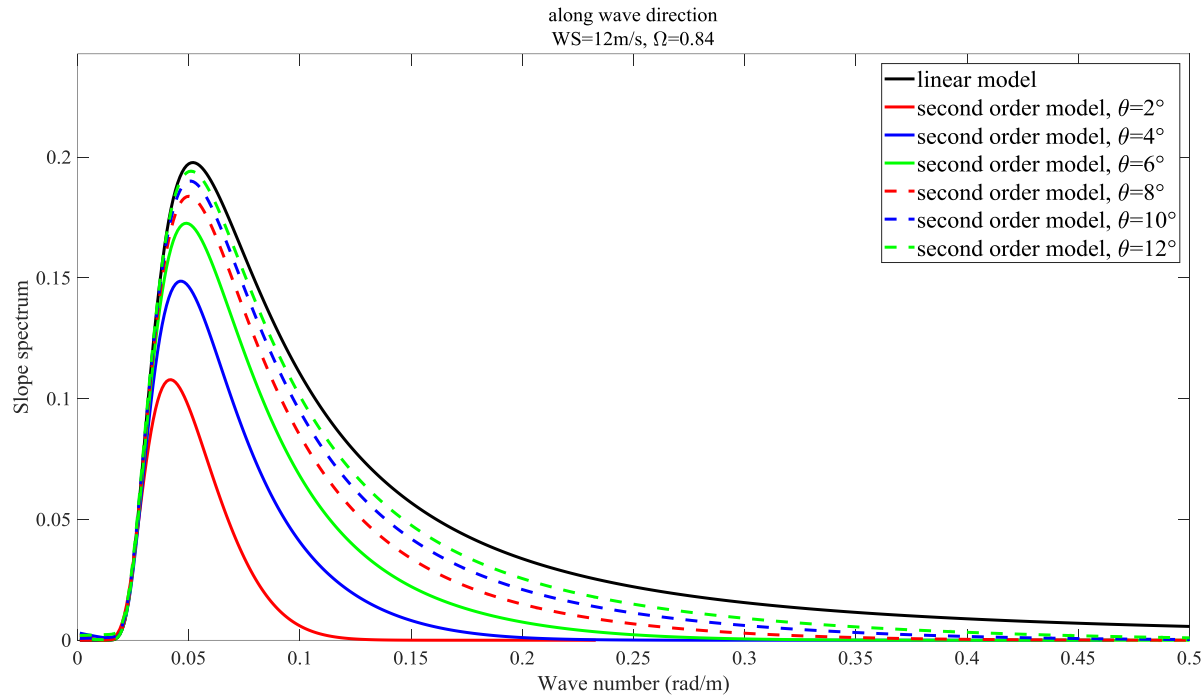


mature wind wave

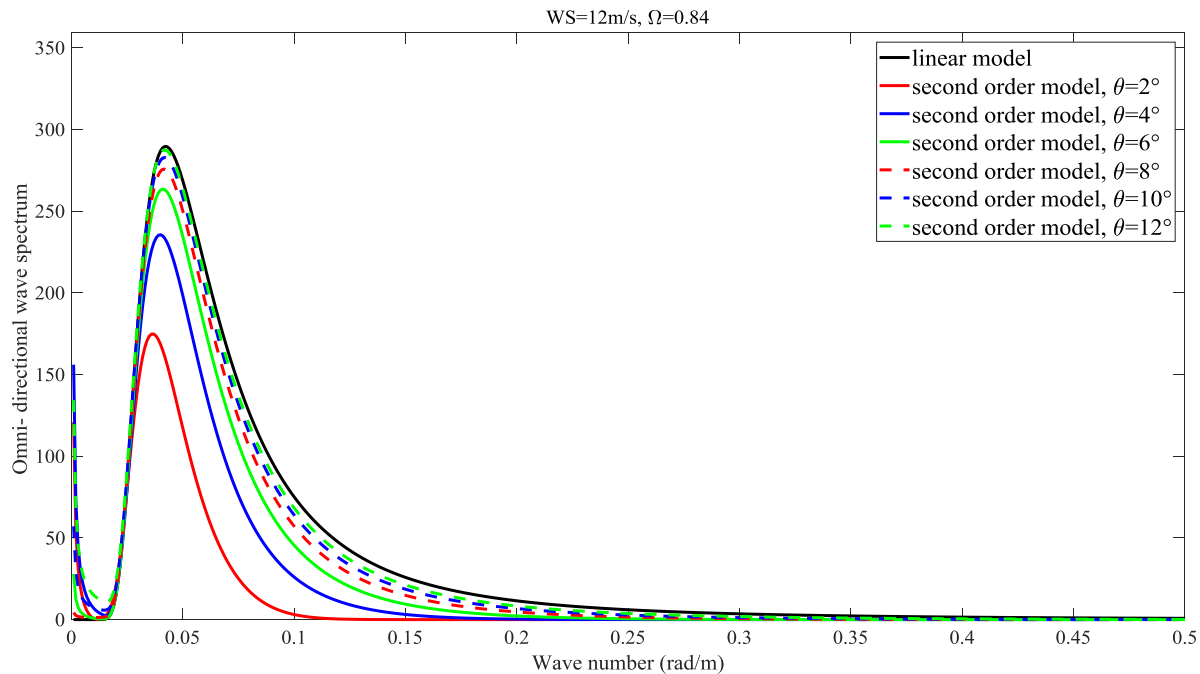
$$U_{10} = 12 \text{ m/s} \quad \Omega = 1$$

	Inversed Hs (m)	Relative error (%)	Inversed λ_p (m)	Relative error (%)
Linear model	2.51	~	95.2	~
2°	1.38	- 45.0	116.4	+ 22.3
4°	1.83	- 27.1	103.0	+ 8.2
6°	2.07	- 17.5	99.7	+ 4.7
8°	2.22	- 11.6	96.7	+ 1.6
10°	2.33	- 7.2	96.7	+ 1.6
12°	2.42	- 3.6	96.7	+ 1.6

Observed along
the wave
direction



Omnidirectional
wave height
spectrum

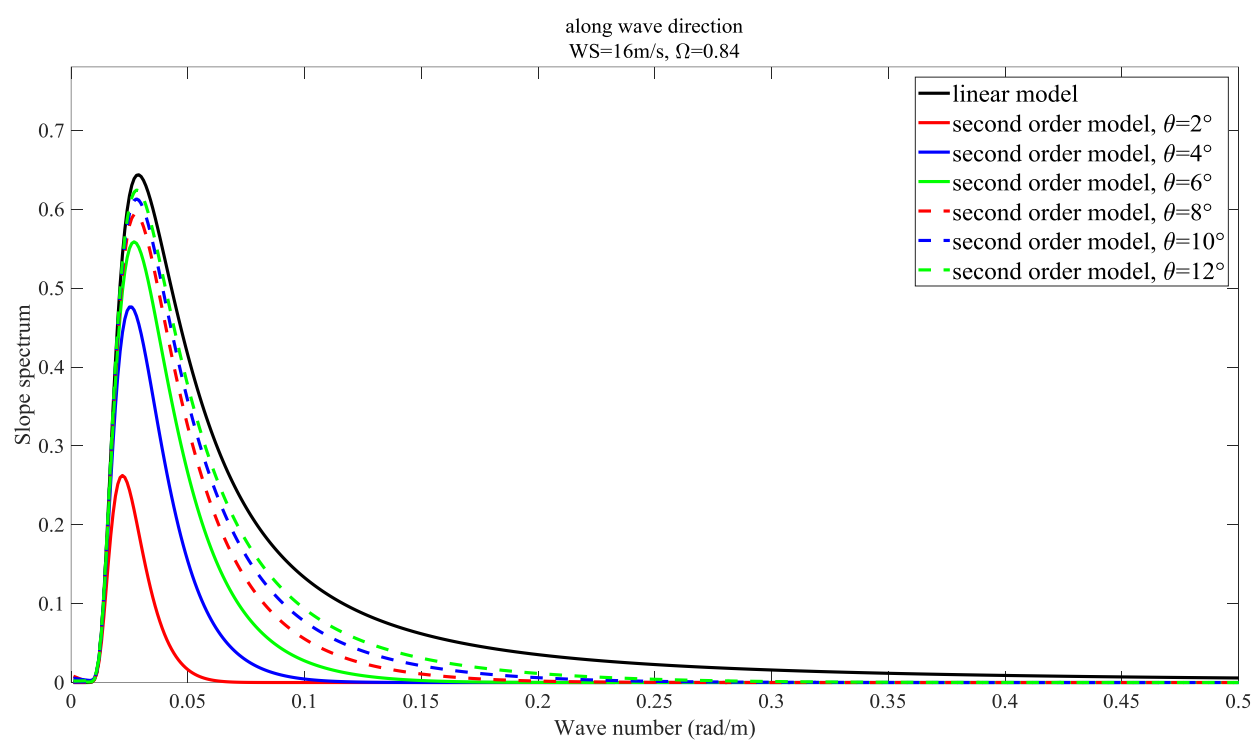


developed wind wave

$$U_{10} = 12 \text{ m/s} \quad \Omega = 0.84$$

	Inversed Hs (m)	Relative error (%)	Inversed λ_p (m)	Relative error (%)
Linear model	3.20	~	149.6	~
2°	1.85	- 42.2	174.5	+ 16.6
4°	2.44	- 23.8	157.1	+ 5.0
6°	2.72	- 15.0	153.2	+ 2.4
8°	2.89	- 9.7	149.6	0
10°	3.02	- 5.6	149.6	0
12°	3.12	- 2.5	149.6	0

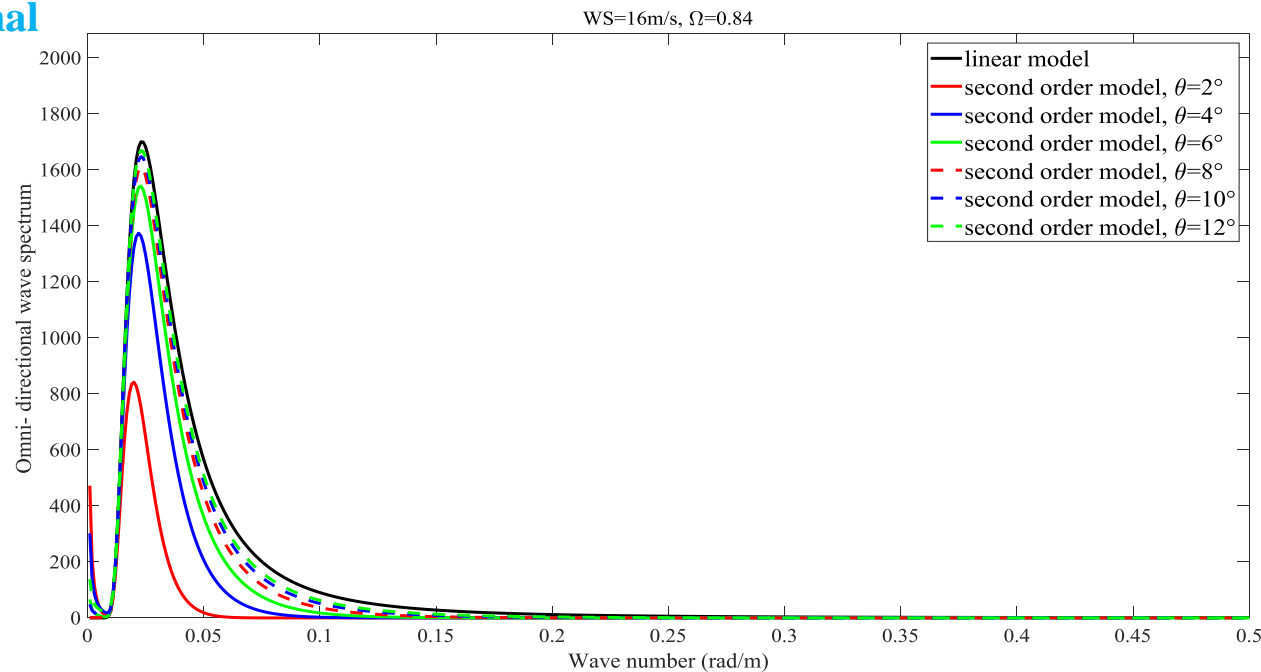
Observed along
the wave
direction



developed wind wave

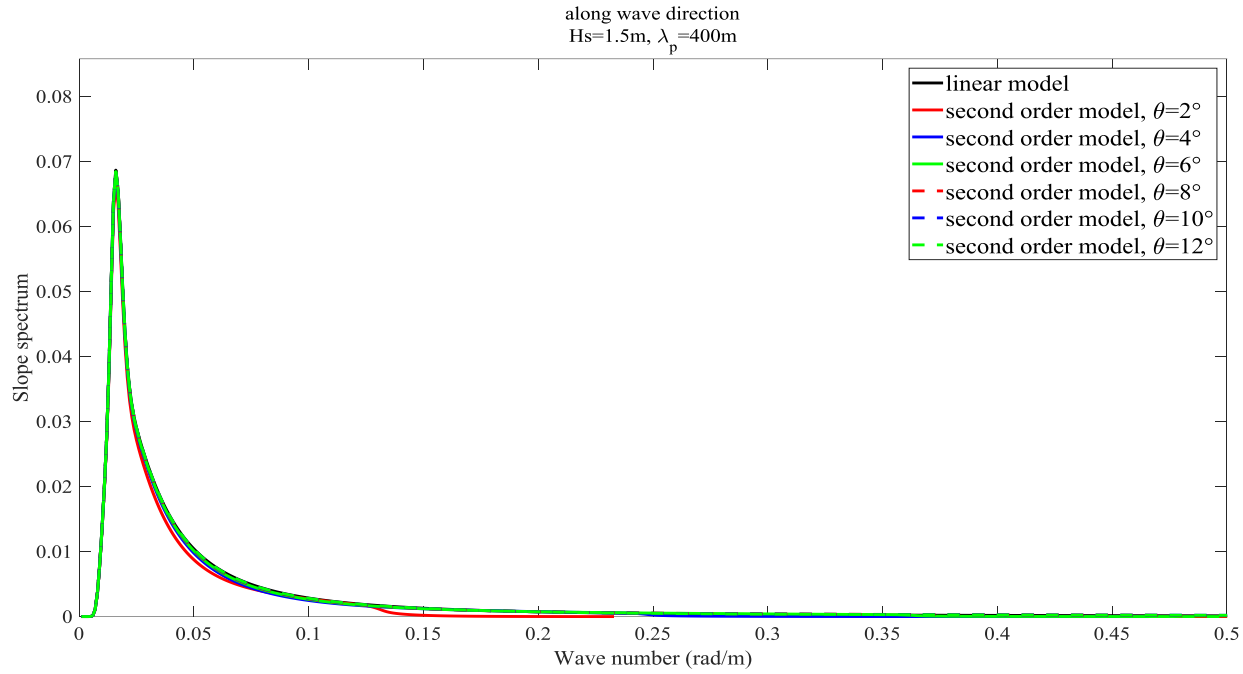
$$U_{10} = 16 \text{ m/s} \quad \Omega = 0.84$$

Omnidirectional
wave height
spectrum



	Inversed Hs (m)	Relative error (%)	Inversed λ_p (m)	Relative error (%)
Linear model	5.77	~	273.2	~
2°	2.88	- 50.1	314.2	+ 15.0
4°	4.28	- 25.8	285.6	+ 4.5
6°	4.85	- 15.9	273.2	0
8°	5.16	- 10.6	273.2	0
10°	5.35	- 7.3	273.2	0
12°	5.49	- 4.9	273.2	0

Observed along
the wave
direction

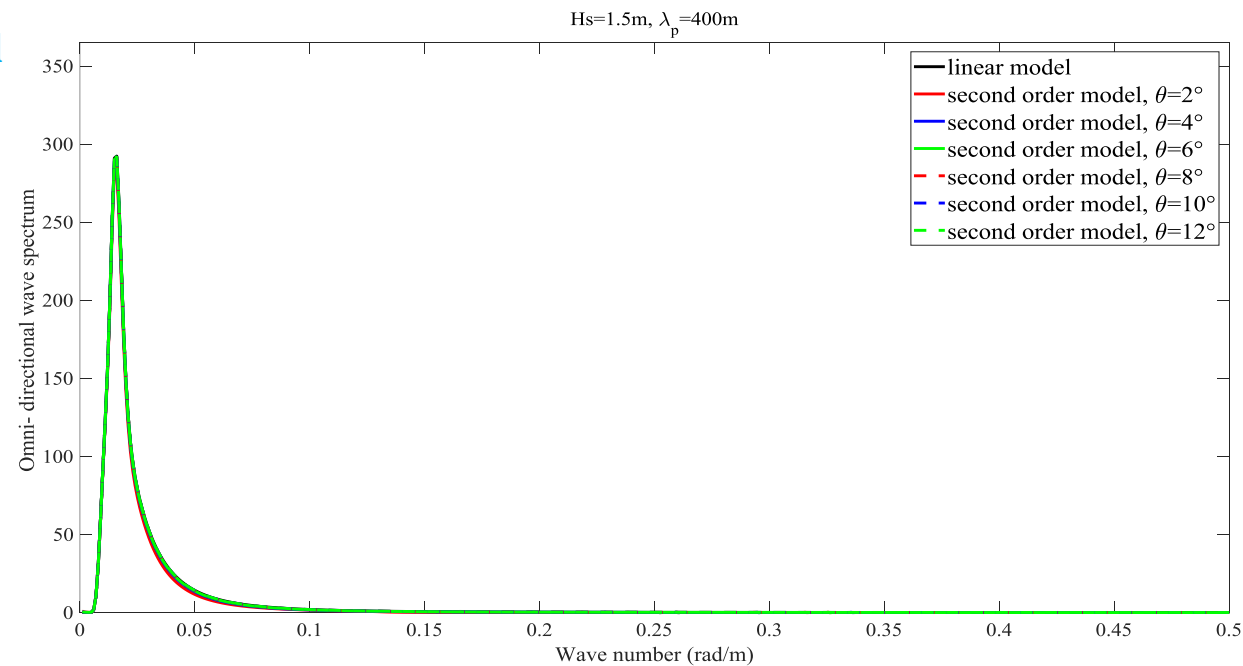


Swell

$H_s = 1.5 m$

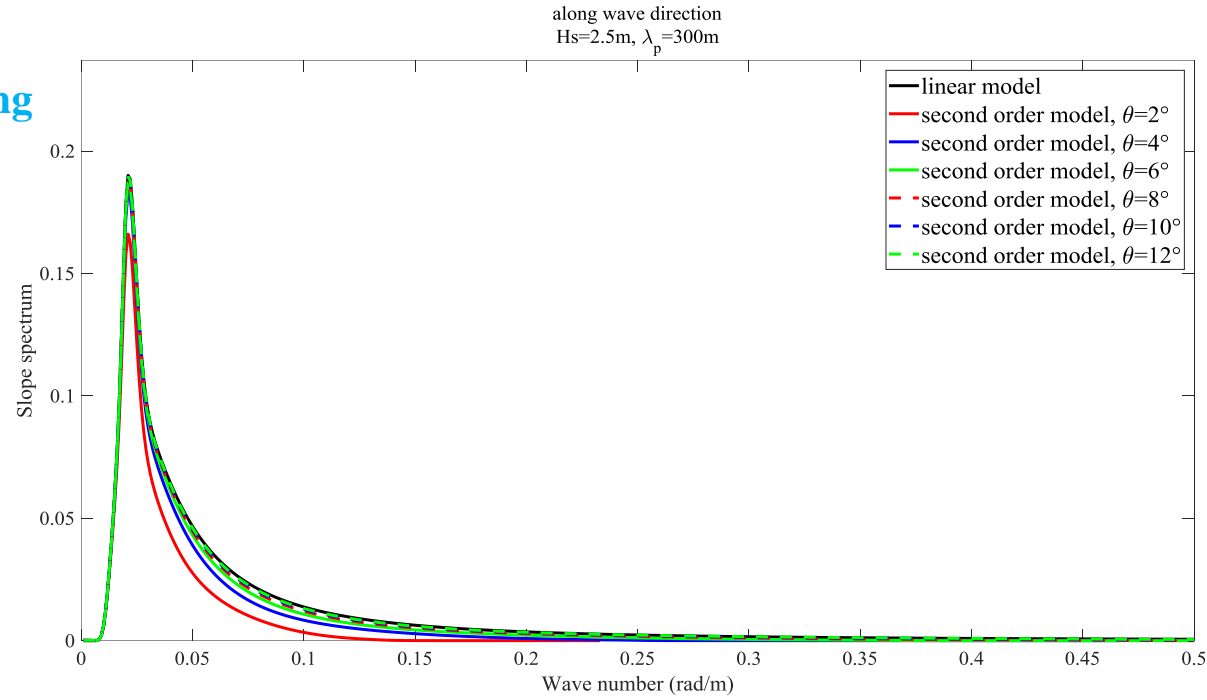
$\lambda_p = 400 m$

Omnidirectional
wave height
spectrum



	Inversed H_s (m)	Relative error (%)	Inversed λ_p (m)	Relative error (%)
Linear model	1.50	~	392.7	~
2°	1.45	- 3.3	392.7	0
4°	1.48	- 1.3	392.7	0
6°	1.49	- 0.7	392.7	0
8°	1.50	0	392.7	0
10°	1.50	0	392.7	0
12°	1.50	0	392.7	0

Observed along
the wave
direction

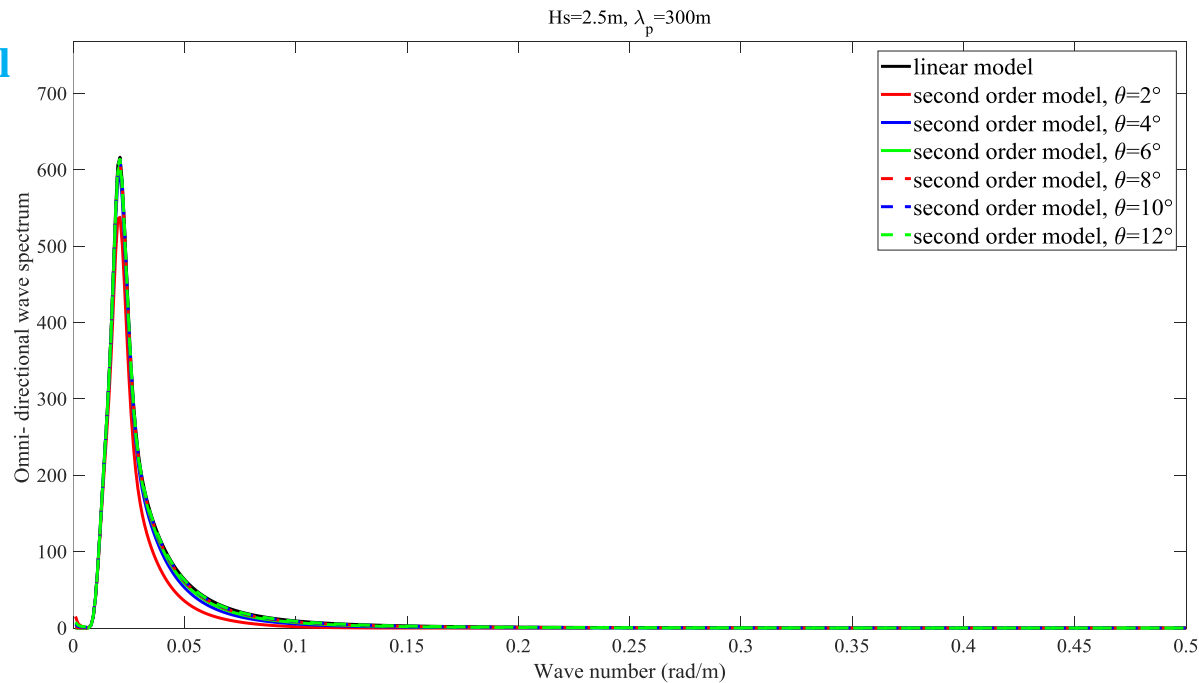


Swell

$$H_s = 2.5 \text{ m}$$

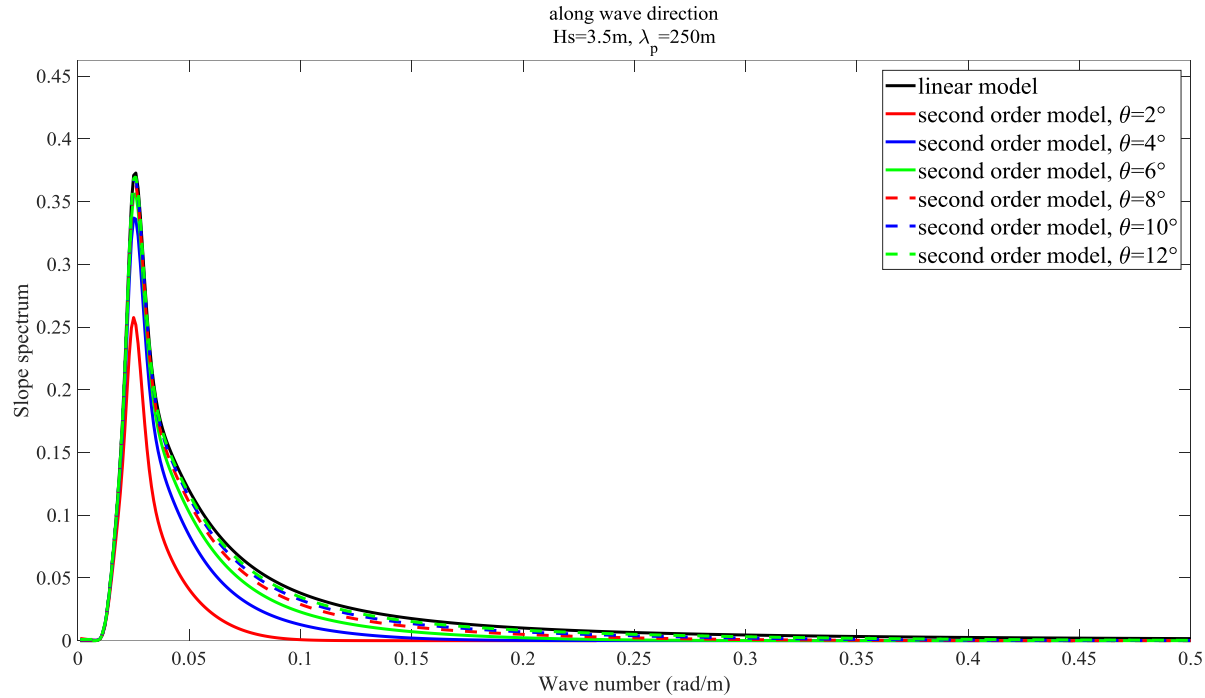
$$\lambda_p = 300 \text{ m}$$

Omnidirectional
wave height
spectrum

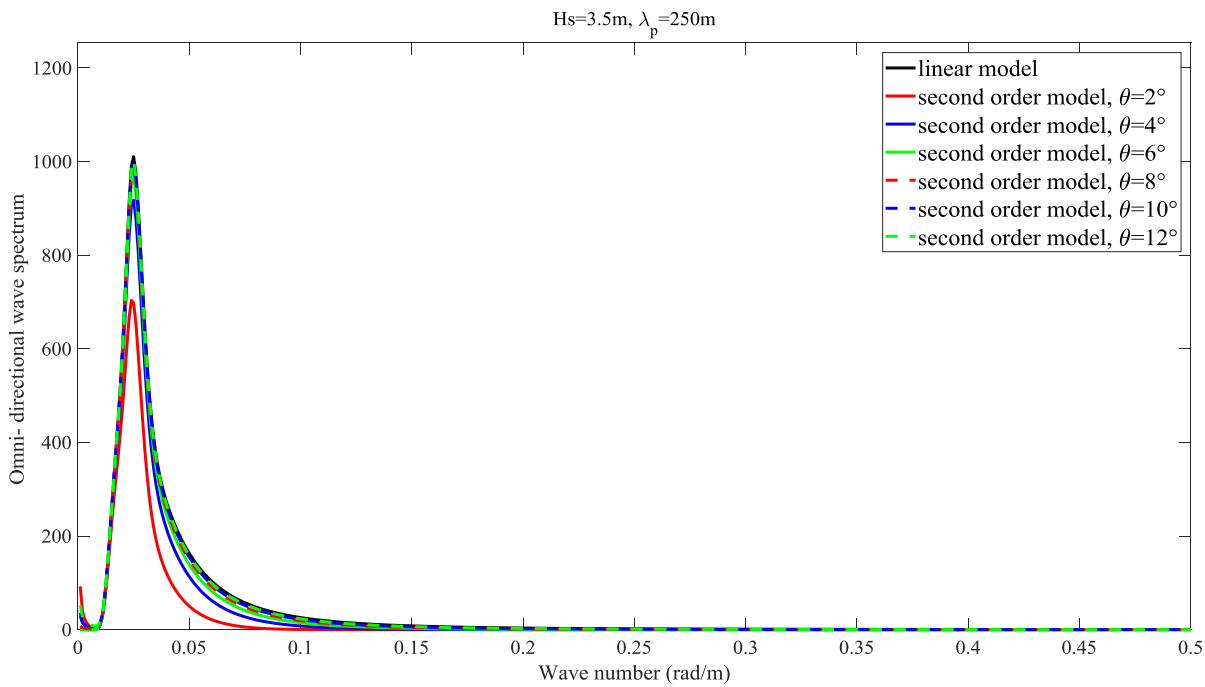


	Inversed H_s (m)	Relative error (%)	Inversed λ_p (m)	Relative error (%)
Linear model	2.51	~	299.2	~
2°	2.17	- 13.5	299.2	0
4°	2.37	- 5.6	299.2	0
6°	2.44	- 2.8	299.2	0
8°	2.47	- 1.6	299.2	0
10°	2.48	- 1.2	299.2	0
12°	2.49	- 0.8	299.2	0

Observed along
the wave
direction



Omnidirectional
wave height
spectrum



Swell

$H_s = 3.5 \text{ m}$

$\lambda_p = 250 \text{ m}$

	Inversed Hs (m)	Relative error (%)	Inversed λ_p (m)	Relative error (%)
Linear model	3.51	~	251.3	~
2°	2.56	- 27.1	261.8	+ 4.2
4°	3.11	- 11.4	251.3	0
6°	3.29	- 6.3	251.3	0
8°	3.38	- 3.7	251.3	0
10°	3.43	- 2.3	251.3	0
12°	3.47	- 1.1	251.3	0

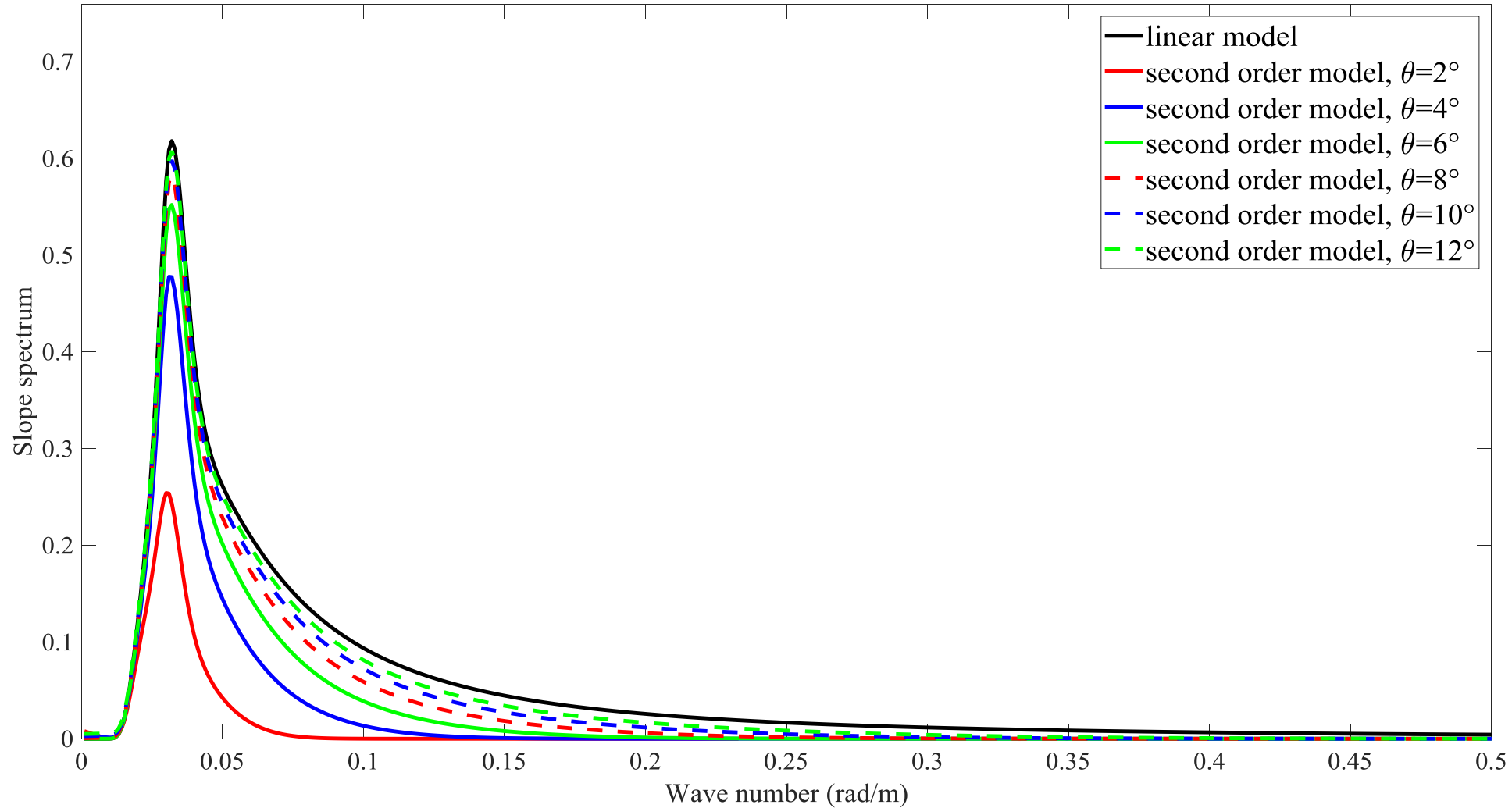
Observed along the wave direction

Swell

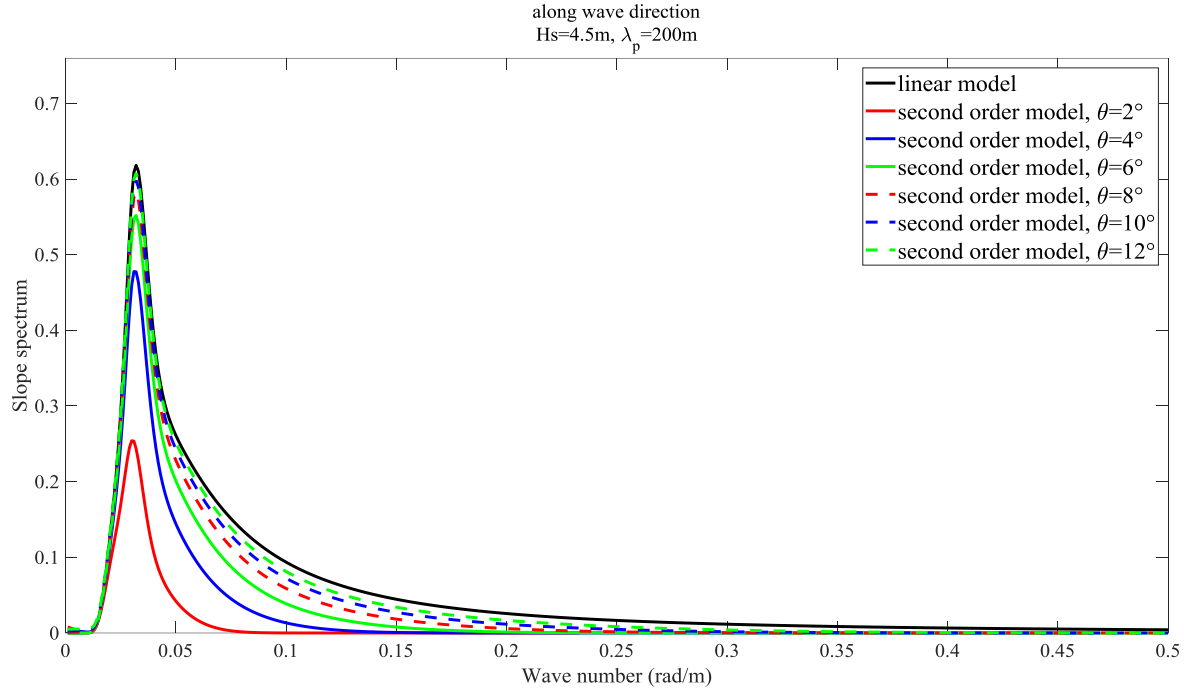
$H_s = 4.5 \text{ m}$

$\lambda_p = 200 \text{ m}$

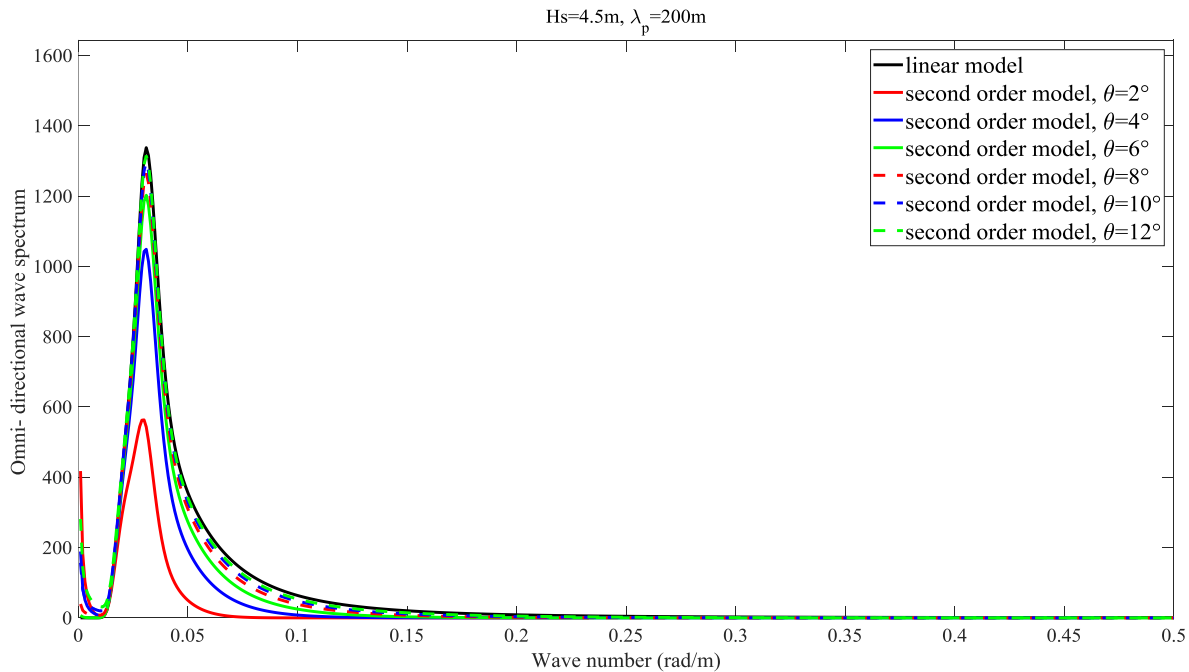
along wave direction
 $H_s=4.5\text{m}, \lambda_p=200\text{m}$



Observed along
the wave
direction



Omnidirectional
wave height
spectrum



Swell

$$H_s = 4.5 \text{ m}$$

$$\lambda_p = 200 \text{ m}$$

	Inversed H_s (m)	Relative error (%)	Inversed λ_p (m)	Relative error (%)
Linear model	4.51	~	202.7	~
2°	2.52	- 44.1	209.4	+ 3.3
4°	3.55	- 21.3	202.7	0
6°	3.94	- 12.6	202.7	0
8°	4.17	- 7.5	202.7	0
10°	4.32	- 4.2	202.7	0
12°	4.43	- 1.8	202.7	0

Conclusion

The effects of range bunching are studied by a theoretical nonlinear modulation model.

The range bunching will lead to the attenuation in the wave number domain where useful signal covers, in meanwhile, also lead to parasitic peaks at low wave number in modulation spectrum.

The effects of range bunching will be pronounced decreasing the incidence angle, increasing wind speed, increasing H_s .

Range-bunching is an important factor leading to

- parasitic peaks at low wave number in inverted wave height spectrum
- Underestimation of inverted H_s under large sea surface conditions